RESEARCH ARTICLE

WILEY

Mapping hippocampal glutamate in mesial temporal lobe epilepsy with glutamate weighted CEST (GluCEST) imaging

Alfredo Lucas[1,2] | Ravi Prakash Reddy Nanga[3] | Peter Hadar[2,4] | Stephanie Chen[5] | Adam Gibson[6] | Kelly Oechsel[7] | Mark A. Elliott[3] | Joel M. Stein[8] | Sandhitsu Das[4] | Ravinder Reddy[3] | John A. Detre[3,4,8] | Kathryn A. Davis[1,4]

[1]Department of Bioengineering, University of Pennsylvania, Philadelphia, Pennsylvania, USA

[2]University of Pennsylvania Perelman School of Medicine, Philadelphia, Pennsylvania, USA

[3]Center for Advanced Metabolic Imaging in Precision Medicine, University of Pennsylvania Perelman School of Medicine, Philadelphia, Pennsylvania, USA

[4]Department of Neurology, University of Pennsylvania Perelman School of Medicine, Philadelphia, Pennsylvania, USA

[5]Department of Neurology (work conducted while at the University of Pennsylvania), University of Maryland School of Medicine, Philadelphia, Pennsylvania, USA

[6]Virginia Commonwealth University School of Medicine (work conducted while at the University of Pennsylvania), Philadelphia, Pennsylvania, USA

[7]Wake Forest University School of Medicine (work conducted while at the University of Pennsylvania), Philadelphia, Pennsylvania, USA

[8]Department of Radiology, University of Pennsylvania Perelman School of Medicine, Philadelphia, Pennsylvania, USA

Correspondence
Kathryn A. Davis, Department of Neurology, University of Pennsylvania Perelman School of Medicine, Philadelphia, Pennsylvania, USA.
Email: katedavis@pennmedicine.upenn.edu

Abstract

Temporal lobe epilepsy (TLE) is one of the most common subtypes of focal epilepsy, with mesial temporal sclerosis (MTS) being a common radiological and histopathological finding. Accurate identification of MTS during presurgical evaluation confers an increased chance of good surgical outcome. Here we propose the use of glutamate-weighted chemical exchange saturation transfer (GluCEST) magnetic resonance imaging (MRI) at 7 Tesla for mapping hippocampal glutamate distribution in epilepsy, allowing to differentiate lesional from non-lesional mesial TLE. We demonstrate that a directional asymmetry index, which quantifies the relative difference between GluCEST contrast in hippocampi ipsilateral and contralateral to the seizure onset zone, can differentiate between sclerotic and non-sclerotic hippocampi, even in instances where traditional presurgical MRI assessments did not provide evidence of sclerosis. Overall, our results suggest that hippocampal glutamate mapping through GluCEST imaging is a valuable addition to the presurgical epilepsy evaluation toolbox.

KEYWORDS
hippocampus, lateralization, neuroimaging, presurgical, sclerosis

1 | INTRODUCTION

Approximately 1.2% of the US population suffers from active epilepsy (Zack & Rosemarie, 2017), that is, patients are either currently taking medication to control it, or had one or more seizures in the past year. Furthermore, recent studies have shown that people with epilepsy have 11 times higher odds of premature death compared with matched controls (Bauman & Devinsky, 2021; Fazel et al., 2013). Epilepsy classification is critical for surgical planning and appropriate pharmacological treatment. In 2017, the International League Against Epilepsy (ILAE) described four main types of epilepsy: focal, generalized, combined generalized and focal, and unknown (Scheffer et al., 2017). Each of those subtypes can then be further subdivided by their etiology, and if focal, by their localization. One of the most common subtypes of focal epilepsy is temporal lobe epilepsy (TLE) (Téllez-Zenteno & Hernández-Ronquillo, 2011). Within TLE, if seizures are identified as originating from the lateral or temporal poles, the term neocortical temporal lobe epilepsy (nTLe) is utilized (Berg et al., 2010; Téllez-Zenteno & Hernández-Ronquillo, 2011). If seizures are identified as originating from the amygdalo-hippocampal area, the term mesial temporal lobe epilepsy (MTLe) is utilized (Berg et al., 2010; Téllez-Zenteno & Hernández-Ronquillo, 2011). Furthermore, within MTLe, the presence of sclerosis and/or atrophy of the hippocampus, termed mesial temporal sclerosis (MTS) or MTLe with hippocampal sclerosis (MTLe-HS), is one of the main causes of drug resistant epilepsies referred for surgery, with high likelihood of post-surgical seizure freedom (Asadi-Pooya et al., 2017; Elsharkawy et al., 2009; Wieser et al., 2004). Some clinicians make a distinction between MTS and MTLe-HS, in that changes in other mesial temporal structures beyond the hippocampus are observed in MTS. However, the terms are often used interchangeably (Thom, 2014). In this study, we use the term lesional MTLe (MTLe-L) to refer to patients that have either histopathological evidence of HS, qualitative and quantitative (i.e., hippocampal volumetry) findings of HS, or both. Furthermore, we use the term non-lesional MTLe (MTLe-NL) to refer to patients that do not have evidence of hippocampal sclerosis.

MTS is characterized pathologically by neuronal loss and astrocyte gliosis, with changes classically seen most prominently in the cornu ammonis 1 (CA1) hippocampal subfield, and the dentate gyrus (DG) (Thom, 2014). Compared with other etiologies of epilepsy, patients with MTS are more likely to be medically refractory, with only 25–42% of patients being controlled on antiepileptic drugs alone (Stephen et al., 2001). Fortunately, MTS is associated with a favorable surgical outcome: 60–80% of patients are seizure-free after temporal lobectomy (Elsharkawy et al., 2009; Wieser et al., 2004), placing significant clinical value in correctly identifying MTS during presurgical evaluation. Recently, there has been an increase in the usage of minimally invasive laser interstitial thermal therapy (LITT) in the treatment of both lesional and non-lesional MTLe (Kang et al., 2016; Le et al., 2018). Appropriate localization of ablation targets within the hippocampus with noninvasive imaging could minimize unnecessary tissue ablation, obviate the need for intracranial electroencephalogram (EEG), and potentially improve the likelihood of post-surgical seizure freedom.

Our group has previously demonstrated that a novel 7 Tesla magnetic resonance glutamate imaging technique, GluCEST (glutamate-weighted chemical exchange saturation transfer) (Cai et al., 2012), can lateralize the epileptic focus in non-lesional epilepsy patients (Davis et al., 2015; Hadar et al., 2021). The objective of this study was to apply this imaging technique to medically refractory TLE patients to further map the spatial distribution of glutamate changes in lesional MTLe patients, and contrast the findings with those in a non-lesional MTLe patient population. We also aimed to better define the utility of GluCEST in lateralizing and differentiating lesional from non-lesional MTLe.

2 | METHODS

2.1 | Patient selection

This study was conducted under an approved Institutional Review Board protocol at the University of Pennsylvania. Presurgical mesial temporal lobe epilepsy patients ($n = 14$) were recruited from the Penn Epilepsy Center. Inclusion criteria included age ≥ 18 years, confirmation of mesial temporal lobe epilepsy diagnosis by scalp EEG, clinical MRI scan, and refractory epilepsy despite adequate trials of at least two anti-seizure medications. We based our group definitions (MTLe-L vs. MTLe-NL) on the clinical consensus from our epilepsy surgical conference, radiological reads, and histopathology, when available. In addition, we used quantitative evidence from hippocampal volumetry, to corroborate our lateralization and group assignments. Hippocampal volume has been shown to be an excellent predictor of hippocampal sclerosis (Bernasconi, 2006; Princich et al., 2021). In order of importance, we considered histopathology first. In the absence of histopathology supporting MTS, the radiological read was considered. In the absence of radiologically evident MTS, hippocampal volumetry was considered, with a hippocampal absolute asymmetry larger than 5.4% (maximum asymmetry in our control population), considered evidence of hippocampal atrophy. Meeting any of the above criteria resulted in a subject defined as MTLe-L, whereas absence of any of the above criteria resulted in a subject defined as MTLe-NL. Exclusion criteria included prior intracranial surgical intervention, contraindications to 7 T MRI scanning (e.g., metallic implant, claustrophobia), and pregnancy. Ten healthy control subjects (three male, aged 23 to 54 years; seven female, aged 24 to 56 years) were also recruited.

2.2 | Patient demographics

Ten MTLe-L, four MTLe-NL, and 10 healthy controls were included in the analysis. Detailed information for each patient can be found in Table 1. All of the included epilepsy patients had medically refractory epilepsy and underwent routine presurgical evaluation, which included confirmation of seizure localization with scalp EEG with video, clinical 3 T brain MRI, and FDG-PET.

TABLE 1 Subject demographics, GluCEST DAI and volumetric DAI for patient cohort

Patient ID	Age	Seizure duration	Seizure localization	MRI brain	PET	Surgery	Pathology	Outcome	Group	GluCEST modality	Hippocampal GluCEST DAI	Hippocampal volume DAI
P007	55F	5 years	Right	R MTS	R temporal hypometabolism	R temporal lobectomy	MTS	Engel IA	MTLe-L	2D	−0.0349	−0.2770
P010	61F	40 years	Left	L MTS	L temporal hypometabolism	L temporal laser ablation	NA	Engel IA	MTLe-L	2D	−0.1263	−0.2711
P012	59F	6 years	Right	R MTS	Unremarkable	R temporal laser ablation	NA	Engel IA	MTLe-L	2D	−0.0076	−0.0274
P015	47F	20 years	Left	L MTS	L anterior and mesial temporal hypometabolism	L temporal lobectomy	MTS	Engel IA	MTLe-L	2D	−0.0441	−0.3347
P019	56F	8 years	Suspected left	Probable L MTS	Left temporal hypometabolism	No surgery	NA	NA	MTLe-L	3D	−0.0976	−0.2434
P021	38 M	12 years	Right	Non-lesional	R anterior hypometabolism	R partial temporal lobectomy	MTS	Engel IA	MTLe-L	3D	−0.1949	0.1166
P025	36 M	31 years	Right	Non-lesional	R temporal hypometabolism	R amygdalo-hippocampectomy	MTS	Engel IA	MTLe-L	3D	−0.0473	−0.3878
P029	40F	16 years	Left	Non-lesional	Left anterior temporal hypometabolism	L temporoamygdalo hippocampectomy	Mild hippocampal sclerosis	Engel IB	MTLe-L	3D	−0.0347	−0.0010
P046	31F	15 years	Left	Probable L MTS	L anterolateral temporal hypometabolism	2 L temporal laser ablation	NA	Engel IA	MTLe-L	2D	−0.0676	−0.1094
P064	56 M	3 years	Left	L MTS	Bilateral temporal hypometabolism	L temporal laser ablation	NA	Engel IIIA	MTLe-L	2D	0.0284	−0.1538
P023	40 M	5 years	Left	Non-lesional	Left medial temporal hypometabolism	NA	NA	NA	MTLe-NL	3D	0.0480	0.0070
P026	32F	4 years	Left	Non-lesional	Unremarkable	NA	NA	NA	MTLe-NL	3D	0.0357	−0.0070
P051	25 M	6 years	Right	Non-lesional	Right mesial temporal hypometabolism	R Temporal laser ablation	NA	Engel IA	MTLe-NL	2D	0.0915	−0.0110
P070	29 M	10 years	Left	Non-lesional	Left temporal hypometabolism	2 L Temporal laser ablations	NA	Engel IIIA	MTLe-NL	2D	0.0125	−0.0450

Abbreviations: MTLe-NL, non-lesional mesial temporal lobe epilepsy; MTLe-L, lesional mesial temporal lobe epilepsy; MTS, mesial temporal sclerosis.

In the MTLe-L group, 8/10 subjects had either confirmed histopathology or a definitive radiological read of MTS. The remaining 2/10 MTLe-L subjects had suspected MTS per radiological read, which was later corroborated in laterality and degree by hippocampal volumetric asymmetry above 5.4%. The four subjects not included in the MTLe-L group had no histopathology available, however, they also had no evidence of sclerosis on imaging, and had hippocampal volumetric asymmetries within the range of our control subjects, therefore they were assigned to the MTLe-NL group. In the MTLe-NL group, 2/4 subjects were part of our previous 3D GluCEST study.

2.3 | MRI scans and data analysis

2.3.1 | Image acquisition

GluCEST MRI was acquired on 7 T whole-brain MRI scanner (Siemens Medical Systems) with a single-channel transmit/32-channel receive proton head phased-array volume coil. The structural 7 T MRI protocol was as described in prior work (Davis et al., 2015; Hadar et al., 2021), and consisted of T_1-weighted anatomical magnetization-prepared rapid gradient echo (MPRAGE) images of the whole brain (176 axial slices, repetition-time/echo-time/inversion-time [TR/TE/TI] = 2800/4.4/1500 ms, flip-angle = 7°, $0.8 \times 0.8 \times 0.8$ mm^3 resolution, iPAT = 2, scan-time 4 m:43 s), T_2-weighted MRI using the variable flip angle turbo spin echo (TSE_VFL) sequence (224 coronal slices, TR/TE = 3000/388 ms, $0.4 \times 0.4 \times 1.0$ mm^3 resolution, iPAT = 2, scan-time 7 m:42 s) followed by the acquisition of the GluCEST sequences. GluCEST acquisition parameters followed those reported for 2D GluCEST (Davis et al., 2015) and 3D GluCEST (Hadar et al., 2021) in prior studies. The 2D GluCEST acquisition, consisted of a single 5 mm slice perpendicular to the long axis of the hippocampus with an in-plane resolution of 0.8×0.8 mm^2. The 3D volumetric GluCEST acquisition, consisted of a partial 3D technique with 60, 1 mm isotropic coronal slices with complete antero-posterior coverage of the hippocampus. In addition, B_0 and B_1 maps of the same slices were acquired and were used to correct B_0 and B_1 inhomogeneities in the 2D and 3D volumetric GluCEST maps, as described previously (Cai et al., 2012). Only 2D GluCEST acquisitions were available for our control population.

2.3.2 | Hippocampal subfield segmentation

The Automated Segmentation of Hippocampal Subfields (ASHS) algorithm (Yushkevich et al., 2006; Yushkevich et al., 2015) was utilized to generate subfield segmentations. Segmentations of bilateral hippocampal subfields (CA1, CA2, CA3, CA4/DG [dentate gyrus]) and hippocampal tail were obtained from 7 T T_2-weighted MRI images similar to our previous work (Shah et al., 2018). Due to their small size, CA2 and CA3 segmentations were combined. The whole hippocampal segmentation was derived by combining the individual subfield segmentations. These segmentations were subsequently resliced into the

single 2D GluCEST slice and into the 3D GluCEST space for 2D and 3D GluCEST analyses, respectively. The 2D and 3D GluCEST maps did not require registration to the structural scans from which the segmentation was derived because their acquisition was immediately after the structural sequences, and the subjects experienced minimal movement between scans. Reslicing of the segmentations into their corresponding 2D and 3D GluCEST space was done using the C3D package distributed with ITK-SNAP (Yushkevich et al., 2006). Using the segmentations as a mask, the average GluCEST contrast within each subfield and across the entire hippocampus was measured. For the subjects with 3D GluCEST, an average across the entire volume of the segmentation mask was used. For subjects with 2D GluCEST, an average across the entire area of the segmentation in the 2D slice was used.

2.3.3 | Directional asymmetry calculation

Hippocampal measurements were divided into ipsilateral and contralateral based on the lateralization of the epileptic seizure onset zone as determined by pre-surgical evaluation. Control subjects' hippocampi were randomly assigned into ipsilateral or contralateral in equal proportion to the MTLe-NL and MTLe-L subjects' lateralization. To distinguish increased from decreased GluCEST in the ipsilateral hippocampus, a directional asymmetry index (DAI) instead of the absolute asymmetry index (AI) was calculated as follows for each subject's hippocampal and subfield segmentation:

$$DAI = \frac{CEST_{ipsi} - CEST_{contra}}{CEST_{ipsi} + CEST_{contra}}$$

Under this definition, a negative DAI will suggest decreased GluCEST in the ipsilateral side, or conversely, increased GluCEST in the contralateral side. An analogous calculation was carried out for the ipsilateral and contralateral whole hippocampal volume, obtaining a volumetric DAI. The absolute asymmetry index (AI), where reported, was calculated as the absolute value of the DAI defined above.

2.3.4 | Hippocampal GluCEST asymmetry maps

In order to better visualize the distribution of GluCEST asymmetry in sclerotic hippocampi, we developed a 2D shape-based registration approach for doing a voxelwise GluCEST contrast comparison between ipsilateral and contralateral hippocampi. For MTLe-L and control patients with 2D GluCEST acquisitions, a 2D registration process was carried out to a template hippocampal segmentation from one of our control subjects. This specific template hippocampus segmentation was chosen due to it being a healthy control, and due to the hippocampus being highly symmetric to the contralateral hippocampus. Then, for each patient and control, a symmetric diffeomorphic 2D transformation was carried out between the 2D hippocampal segmentation of each hippocampus (left and right) and

the template hippocampal segmentation described previously. After the registration to the template hippocampus was defined for each subject and each hippocampus, the registration was applied to the GluCEST map masked by the original hippocampal segmentation, resulting in a hippocampal GluCEST map registered to the template hippocampus. Finally, with a GluCEST map of each hippocampus in this template space, the absolute asymmetry (absolute value of the DAI) in GluCEST contrast between left and right hippocampi at each voxel, and for each subject, was calculated. A two-sample t-test was subsequently carried out at every voxel comparing MTLe-L and controls, generating a spatial t-statistic map along the hippocampus. The registration described above was carried out using the Symmetric Normalization (SyN) algorithm proposed by Avants et al. (2008) and implemented in DIPY 1.5.0 in Python 3.8. Only those patients with 2D GluCEST were used for this analysis because of the lack of a control population in the 3D GluCEST dataset.

2.4 | Statistics

A one-way ANOVA with multiple comparisons was carried out to compare the GluCEST DAI as well the hippocampal volume DAI between control, MTLe-L and MTLe-NL subjects for the whole hippocampal segmentation. For the subfield analysis, a two-sample t-test was used to compare the means of each subfield DAI between the MTLe-L and MTLe-NL groups. Bonferroni correction was used for multiple comparisons. 2D and 3D GluCEST whole hippocampus DAI measurements for the MTLe-L group were compared using a non-parametric Mann–Whitney rank test, given the small sample sizes used in this comparison. Statistical significance was defined at $p < .05$. Results are presented as mean ± SEM. Effect sizes, when reported, are reported as Cohen's D values.

3 | RESULTS

3.1 | Whole hippocampus DAI

Figure 1a–c show the 2D distribution of GluCEST in representative control, MTLe-L and MTLe-NL subjects. Individual whole hippocampus mean GluCEST DAI values are shown in Table 1. Out of 10 MTLe-L subjects, nine had a negative DAI, including three subjects with MRI-negative, but pathology confirmed MTLe-L (Patients P021, P025, and P029, Figure 2). The average GluCEST DAI in the whole hippocampus for the MTLe-L, control and MTLe-NL groups were -0.063 ± 0.020, 0.017 ± 0.016, and 0.047 ± 0.017, respectively (Figure 1d). Statistically significant differences were found between the whole hippocampus mean GluCEST DAI of MTLe-L and controls ($p < .01$, corrected. Cohen's D, 1.38), and MTLe-L and MTLe-NL ($p < .01$, corrected. Cohen's D, 2.16). No differences were found between the hippocampal mean GluCEST DAI of control and MTLe-NL subjects ($p = .610$, corrected. Cohen's D, 0.71). No statistically significant differences were found between 2D and 3D whole hippocampus mean GluCEST DAI for the MTLe-L group ($p = .227$), although there was a moderately large effect size, with 3D GluCEST hippocampal DAI having a more negative DAI than 2D GluCEST (Cohen's D,
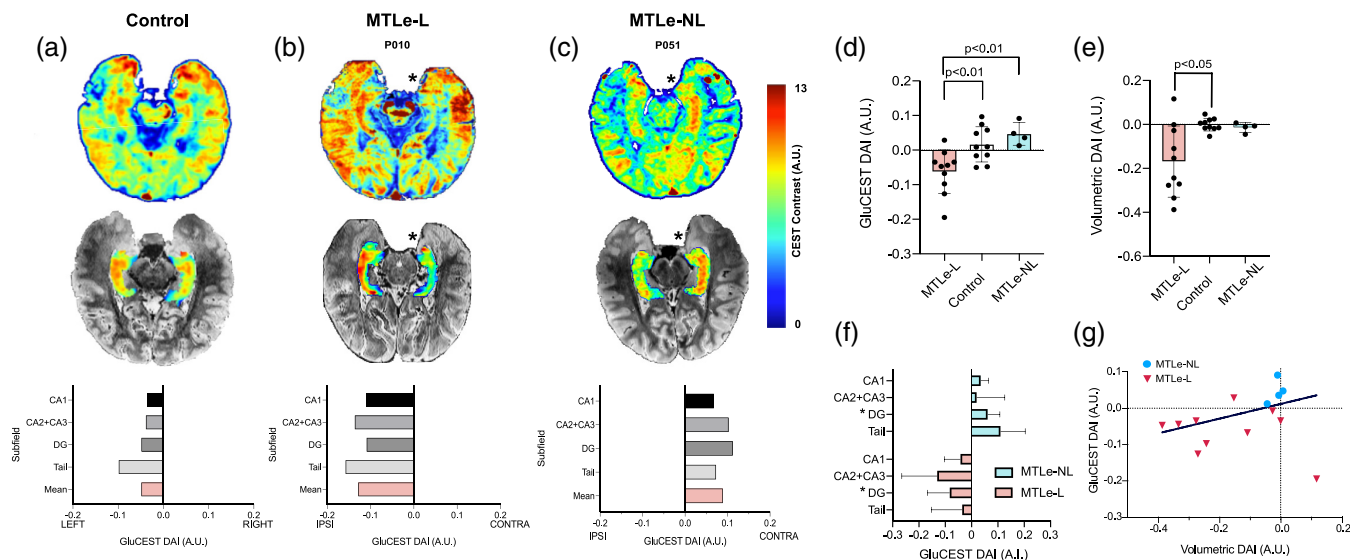
FIGURE 1 (a–c) GluCEST signal varies based on sclerosis. Top: Representative 2D GluCEST slice for a control (a), MTLe-L (b) and MTLe-NL (c) subject. * represents the ipsilateral side based on the lateralization of the epileptic seizure onset zone as determined by pre-surgical evaluation. Subject P051 mirrored for ease of comparison. Middle: The same slice but with only the hippocampal segmentation GluCEST map, overlaid on the T2 structural image. Bottom: GluCEST DAI for each subfield, as well as the mean GluCEST DAI across subfields. (d) Whole hippocampus GluCEST DAI for the three groups. (e) Whole hippocampus volumetric DAI for the three groups. (f). Subfield DAI for the MTLe-L and MTLe-NL groups. * represents that the subfield DAI between the groups is significantly different ($p < .05$). (g) Scatterplot with iteratively reweighted least squares (IRLS) linear fit of volumetric DAI versus GluCEST DAI. A.U., arbitrary units; DAI, directional asymmetry index
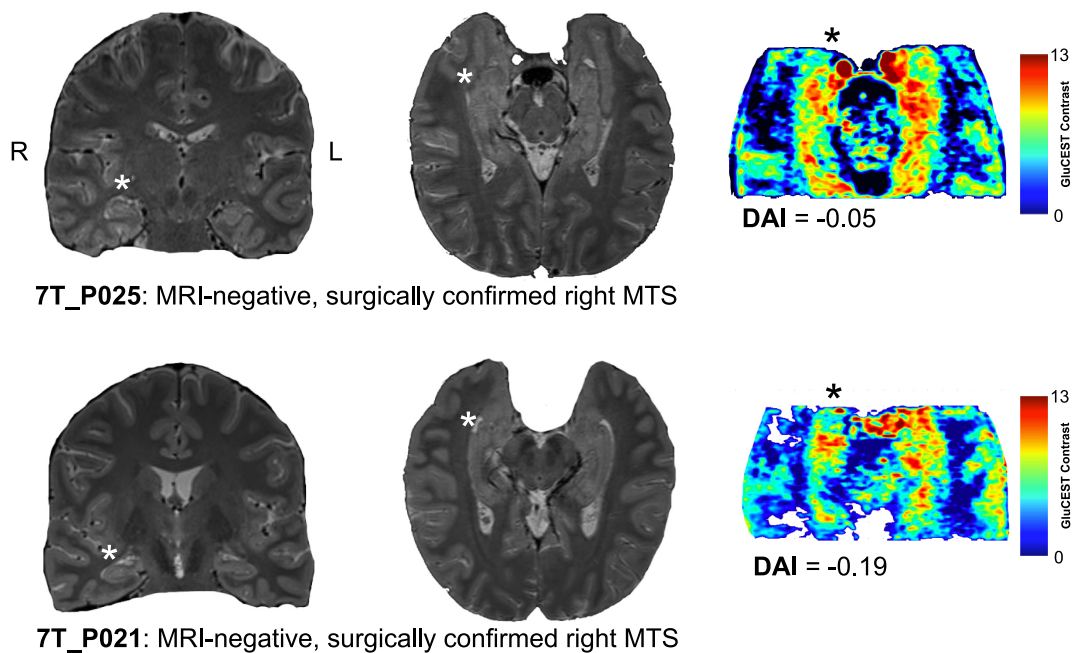
FIGURE 2 GluCEST and MRI comparisons. Coronal (left), and axial (middle) 3T T2w MRI, as well as axial 3D GluCEST slice (right) for two MRI-negative surgically confirmed right MTS patients. Both patients had left sided seizure onset, as represented by the asterisk next to the hippocampus. DAI stands for the GluCEST contrast directional asymmetry index

0.81). A statistical comparison between 2D and 3D GluCEST DAI for the MTLe-NL was not done due to the small sample size, but the values were consistent in range and sign for the two GluCEST acquisition types, with a small effect size when comparing DAI between the two acquisition modalities (Cohen's D, 0.25).

In addition to comparing GluCEST DAI differences with the proposed group assignments of MTLe-L and MTLe-NL, we also compared two other potential group assignments based on the MRI-lesional status and the degree of hippocampal volumetric asymmetry (Figure S1). These alternative group assignments are independent of the presence of histopathology, unlike our original assignments. For the MRI-lesional status assignment (Figure S1A), we found no statistically significant differences between the MRI-positive (MRI+) and the MRI-negative (MRI-) groups ($p = .37$), although there was a moderate effect size, with MRI+ subjects having a more negative GluCEST DAI than MRI- subjects (Cohen's D, 0.54). For the MRI- subjects that had histopathology available (Figure S1B), and hence confirmed MTS, we found a significantly lower GluCEST DAI ($p = .031$. Cohen's D, 2.26), compared with the MRI- subjects without available histopathology. Finally, for the hippocampal volumetric asymmetry group assignment (Figure S1C), subjects with high volumetric asymmetry (more than 5.4%, as defined in the Patient Selection section) had a significantly lower GluCEST DAI ($p = .011$. Cohen's D, 1.80). Overall, these findings suggest that separating the subjects solely based on hippocampal volumetric asymmetry would result in findings that are consistent with the original MTLe-L and MTLe-NL group assignments, without the need for histopathology. On the other hand, separating the groups based on MRI lesional status alone leads to an MRI- group with a wide

distribution of GluCEST DAI values, since that group might contain subjects with and without histopathological MTS.

The volumetric DAIs in the whole hippocampus for the MTLe-L, control and MTLe-NL groups were -0.17 ± 0.05, -0.001 ± 0.009, and -0.014 ± 0.011, respectively (Figure 1e). Statistically significant differences were found between the whole hippocampus volumetric DAI of MTLe-L and controls ($p < .05$, corrected. Cohen's D, 1.44). No differences in volumetric DAI were found between MTLe-NL and controls ($p = .99$, corrected. Cohen's D, 0.51), and MTLe-NL and MTLe-L ($p = .31$, corrected. Cohen's D, 1.34). An apparent positive correlation can be visualized between the volumetric DAI and average GluCEST DAI (Figure 1f). Subject P021 corresponds to the point that falls outside of the general trend of the other subjects (very positive volumetric DAI with negative GluCEST DAI, likely due to non-lesional MRI but pathological MTS). Iteratively reweighted least squares (IRLS) was used to fit a linear model to the data while also taking into account large deviations from the trend. The slope of the model was found to be positive (0.84), but not statistically different from 0 ($p = .10$).

3.2 | Subfield DAI

In addition to trying to quantify the asymmetry of the mean GluCEST in the hippocampus, we wanted to better understand what was the distribution of asymmetries across the hippocampal subfields. The average DAI for each analyzed subfield in the MTLe-NL and MTLe-L groups are shown in Figure 1f. In the MTLe-L group, the average
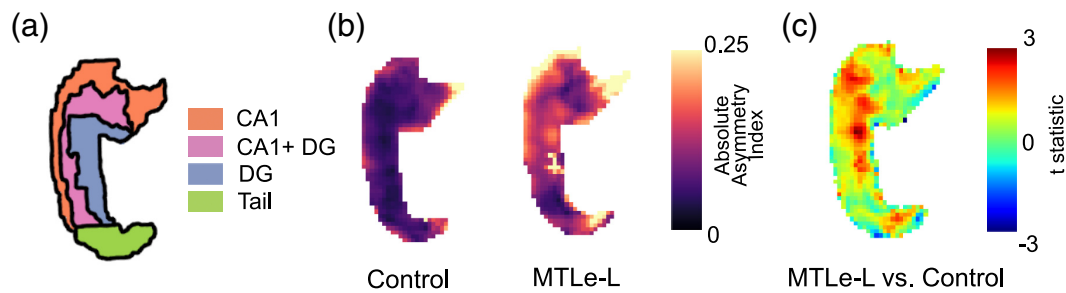
FIGURE 3 2D hippocampal registration results. (a) Shows the distribution of subfields along the hippocampal template used. (b) Shows the absolute asymmetry index (AI) hippocampal maps between left and right hemispheres at each voxel averaged across all subjects for Control and MTLe-L. (c) *t*-statistic comparing the MTLe-L to the control hippocampal maps shown in part B. Positive values represent larger asymmetry in MTLe-L, whereas negative values represent larger asymmetries in controls

subfield DAIs were: −0.043 ± 0.019, −0.129 ± 0.043, −0.084 ± 0.026, −0.036 ± 0.037, for CA1, CA2 + CA3, DG and the hippocampal tail. In the MTLe-NL group, the average subfield DAIs were: 0.036 ± 0.014, 0.020 ± 0.053, 0.062 ± 0.023, and 0.111 ± 0.046, for CA1, CA2 + CA3, DG, and the hippocampal tail. The Cohen's *D* values between MTLe-L and MTLe-NL were 1.68, 1.22, 2.18, 1.39 for CA1, CA2 + CA3, DG, and the hippocampal tail. The DAIs for the DG were significantly different between the two groups ($p < .05$, corrected). This last finding is consistent with the DG being highly glutamatergic (Tamminga et al., 2012) and involved in MTS (Scharfman, 2019). Furthermore, the subfield with the second largest effect size between the groups was CA1, which is the other subfield commonly implicated in MTS (Thom, 2014).

3.2.1 | Hippocampal GluCEST asymmetry maps

Figure 3 shows the results of the 2D hippocampal registration. Figure 3b shows a comparison of the distribution of absolute asymmetries across control and MTLe-L patients. The distribution of asymmetry for controls demonstrates a homogeneous asymmetry across the entire hippocampus. For the MTLe-L patients, we see that the distribution of asymmetry is more heterogeneous, demonstrating increased asymmetry in the region corresponding to the DG, DG +- CA1, CA1 and the hippocampal tail. The statistical map shown in Figure 3c showed a positive t-statistic cluster in the DG and along the DG + CA1/CA1 region, showing that these regions had increased absolute asymmetry in MTLe-L relative to controls.

4 | DISCUSSION

Our findings suggest that GluCEST directional asymmetry differs in MTLe-L versus MTLe-NL. In MTLe-L, the mean GluCEST contrast is lower in the ipsilateral hippocampus, whereas for MTLe-NL patients the concentration is higher in the ipsilateral hippocampus. GluCEST lateralization was also consistent with hippocampal pathology in three subjects who had seemingly non-lesional pathology on MRI but were

later confirmed to have MTS on surgical pathology (Patients P021, P025, and P029 on Table 1 and Figure 2). These findings highlight the potential of GluCEST for detecting MTS in instances where structural MRI is negative.

Glutamate concentration, as measured using magnetic resonance methods, is thought to represent the total parenchymal glutamate pool, including both synaptic and metabolic components (intra- and extracellular) (Cai et al., 2012). Prior work has shown that MTS patients have a 35–40% loss of glutamate synthetase protein and activity in astrocytes of the hippocampus (Eid et al., 2004) when compared with autopsy controls. Magnetic resonance spectroscopy (MRS) studies in humans (Gonen et al., 2020; Pimentel-Silva et al., 2020) have demonstrated *decreased* hippocampal glutamate in MTS ipsilateral to the seizure focus. These findings are consistent with the negative hippocampal DAI observed in the MTLe-L subjects presented in this study. In addition, our results suggest that in the hippocampi, there is an apparent positive correlation between the degree of volumetric asymmetry and the mean GluCEST asymmetry in most MTLe-L subjects, although this is not the case for all subjects. Since we normalize by segmentation volume/area by using mean GluCEST, the volumetric-GluCEST DAI correlation is consistent with the idea that as sclerotic tissue populates the affected hippocampus, the glutamatergic synapses decrease proportionally. Furthermore, it is known that the DG is both highly glutamatergic (Tamminga et al., 2012) and involved in MTS (Scharfman, 2019), which supports the significant difference in DAI observed in the DG between MTLe-L and MTLe-NL.

TLE is increasingly recognized as a heterogeneous disease, and phenotypic differences between different subtypes of TLE have been identified across a range of neuroimaging modalities (Bernhardt et al., 2010; Bernhardt et al., 2015; Shah et al., 2019). The differences between MTLe-L and MTLe-NL hippocampal glutamate concentrations presented in this study further support the disease heterogeneity of TLE, and in particular of mesial temporal lobe epilepsy. Relatedly, our prior work by Shah and colleagues (Shah et al., 2019) demonstrated an analogous pattern of asymmetry in functional connectivity to the one shown by the GluCEST contrast in this study. Shah's study demonstrated a negative functional network directional asymmetry for the MTLe-L subjects and a positive functional

directional asymmetry for the MTLe-NL subjects ipsilateral to the seizure onset zone, as compared with controls. Furthermore, about half of the patients used in that study were also included in this current study. The glutamate concentration asymmetry seen in these two subtypes of TLE might be one of the drivers for the differences in functional asymmetry detected between them.

In this study, we also provided a comparison between GluCEST asymmetry in MTLe-L and controls at a voxel level, by registering control and patient's hippocampi to the same template. With this approach, we were able to obtain the distribution of GluCEST contrast asymmetries at a group level, across the hippocampus. This provides a clear advantage over single voxel MRS strategies (Gonen et al., 2020; Pimentel-Silva et al., 2020), since spatial information can be used for more precise localization of abnormal/sclerotic regions in the hippocampus. While only reported here at the group level, this approach can also be used at the single subject level by coregistering both hippocampi together, showing the distribution of asymmetries for a single subject. It is currently not clear whether the regions with high glutamate asymmetries are necessarily the ones driving epileptogenicity, but longitudinal studies, where GluCEST measurements are done before and after surgical resection or ablation, could help identify whether this is the case. In future studies, colocalization of GluCEST contrast with FLAIR hyperintensities, as well as other structural metrics that correlate with sclerosis, could help spatially distinguish partially sclerotic regions with some glutamatergic activity, from those without glutamatergic activity. As epilepsy surgery becomes less invasive, spatially precise identification and characterization of sclerotic foci could improve surgical outcomes, reduce unnecessary tissue removal, and obviate the need for intracranial EEG in some cases.

7 T imaging has recently been approved for clinical use by regulatory agencies in both the United States and Europe, significantly increasing the incentive for hospitals to adopt this technology (Cosottini & Roccatagliata, 2021). We believe that GluCEST provides a novel, but also highly practical application for 7 T imaging, particularly in the context of epilepsy. However, our GluCEST acquisition approaches are currently restricted to either a single slice, or a limited 3D field of view. Our group is currently working on expanding the GluCEST acquisition to a larger field of view which provides 3D whole brain coverage, expanding the ability to study glutamate distributions across the cerebral cortex in both mesial and extra-mesial temporal lobe epilepsy.

One limitation of this study is that it relies on asymmetry measures. Asymmetry measurements are a common strategy in lateralized epilepsy studies since the contralateral hemisphere provides an internal control for normalizing quantities of interest. Contralateral hippocampal involvement, however, is a well-known phenomenon, even in well lateralized epilepsies (Keller & Roberts, 2008; Liu et al., 2012; Passarelli et al., 2015). Involvement of the contralateral hippocampus in this study could have led to a potentially skewed hippocampal GluCEST contrast and volumetric DAI measurement. Another limitation of this study is that the use of DAI as presented requires a priori knowledge of either the seizure onset lateralization or the epilepsy subtype. However, in combination with clinical evidence, and other

commonly acquired noninvasive testing during epilepsy presurgical evaluation, GluCEST hippocampal asymmetry can be used to confirm the presence of MTS, and potentially to show the distribution of sclerosis in the hippocampus. Accurate pre-surgical distinction between MTLe-NL and MTLe-L using GluCEST has prognostic implications, since the presence of hippocampal sclerosis is one of the most important positive predictive factors for a good surgical outcome (Spencer et al., 2005). Another limitation of this work is the small sample size, particularly in the MTLe-NL group. Fortunately, the increased contralateral GluCEST contrast in the MTLe-NL group has been consistently demonstrated in prior studies from our group in both 2D (Davis et al., 2015) and 3D (Hadar et al., 2021) GluCEST acquisitions. We also acknowledge that our MTLe-NL group is a group assignment of exclusion, and without histopathological confirmation, there is no way of knowing whether our MTLe-NL subjects are truly MTLe-NL. However, our results suggest that if we had defined the lesional and non-lesional status of the subjects based on hippocampal volumetry alone, without incorporating histopathological measurements, our conclusions would have remained the same. This is particularly relevant for future studies since as LITT becomes more common, less histopathological samples will be available, and therefore the definition of lesional and non-lesional MTLe will have to be done exclusively based on MRI. Fortunately, past studies have established that hippocampal volumetry is an excellent predictor of hippocampal sclerosis (Bernasconi, 2006; Princich et al., 2021), therefore as we recruit more subjects for a larger GluCEST study, group assignments will likely be defined by hippocampal volumetry together with MRI lesional status. Future studies from our group aim at acquiring a larger sample size of MTLe-L, MTLe-NL and controls subjects in order to perform a well-powered study where differences between these groups can be explored in both an ROI and voxel-wise fashion without the need for asymmetry measurements. Additionally, subjects will have multimodal imaging data (functional magnetic resonance imaging, diffusion tensor imaging, and arterial spin labeling imaging) which could help elucidate the neurobiological mechanisms that might be driving these changes in glutamate contrast.

5 | CONCLUSION

The results presented in this study suggest that GluCEST hippocampal asymmetry in the form of DAI is negative in MTLe-L and positive in MTLe-NL, and that the magnitude of the DAI correlates with the degree of hippocampal volume loss. These findings provide a complimentary, and necessary, expansion to the current applicability of GluCEST in epilepsy. Our findings further suggest that GluCEST has the potential to contribute to the pre-surgical evaluation of temporal lobe epilepsy by providing noninvasive information about epilepsy subtype, lateralization, as well as distribution of sclerosis.

CONFLICT OF INTEREST

The authors declare no conflict of interest.

DATA AVAILABILITY STATEMENT

The data that support the findings of this study are available from the corresponding author upon reasonable request.

ETHICS STATEMENT

We confirm that we have read the Journal's position on issues involved in ethical publication and affirm that this report is consistent with those guidelines.

ORCID

Alfredo Lucas https://orcid.org/0000-0001-9439-735X
Kathryn A. Davis https://orcid.org/0000-0002-7020-6480

REFERENCES

Asadi-Pooya, A. A., Stewart, G. R., Abrams, D. J., & Sharan, A. (2017). Prevalence and incidence of drug-resistant mesial temporal lobe Epilepsy in the United States. *World Neurosurgery*, 99, 662–666. https://doi.org/10.1016/j.wneu.2016.12.074

Avants, B., Epstein, C., Grossman, M., & Gee, J. (2008). Symmetric diffeomorphic image registration with Cross-correlation: Evaluating automated labeling of elderly and neurodegenerative brain. *Medical Image Analysis*, 12(1), 26–41. https://doi.org/10.1016/j.media.2007.06.004

Bauman, K., & Devinsky, O. (2021). Seizure clusters: morbidity and mortality. *Frontiers in Neurology*, 12. https://doi.org/10.3389/fneur.2021.636045

Berg, A. T., Berkovic, S. F., Brodie, M. J., Buchhalter, J., Cross, J. H., van Emde Boas, W., Engel, J., French, J., Glauser, T. A., Mathern, G. W., Moshé, S. L., Nordli, D., Plouin, P., & Scheffer, I. E. (2010). Revised terminology and concepts for organization of seizures and epilepsies: Report of the ILAE commission on classification and terminology, 2005-2009. *Epilepsia*, 51(4), 676–685. https://doi.org/10.1111/j.1528-1167.2010.02522.x

Bernasconi, A. (2006). Magnetic resonance imaging in intractable epilepsy: Focus on structural image analysis. *Advances in Neurology*, 97, 273–278.

Bernhardt, B. C., Bernasconi, N., Concha, L., & Bernasconi, A. (2010). Cortical thickness analysis in temporal lobe Epilepsy: Reproducibility and relation to outcome. *Neurology*, 74(22), 1776–1784. https://doi.org/10.1212/WNL.0b013e3181e0f80a

Bernhardt, B. C., Hong, S.-J., Bernasconi, A., & Bernasconi, N. (2015). Magnetic resonance imaging pattern learning in temporal lobe epilepsy: Classification and prognostics. *Annals of Neurology*, 77(3), 436–446. https://doi.org/10.1002/ana.24341

Cai, K., Haris, M., Singh, A., Kogan, F., Greenberg, J. H., Hariharan, H., Detre, J. A., & Reddy, R. (2012). Magnetic resonance imaging of glutamate. *Nature Medicine*, 18(2), 302–306. https://doi.org/10.1038/nm.2615

Cosottini, M., & Roccatagliata, L. (2021). Neuroimaging at 7 T: Are we ready for clinical transition? *European Radiology Experimental*, 5(1), 37. https://doi.org/10.1186/s41747-021-00234-0

Davis, K. A., Nanga, R. P. R., Das, S., Chen, S. H., Hadar, P. N., Pollard, J. R., Lucas, T. H., Shinohara, R. T., Litt, B., Hariharan, H., Elliott, M. A., Detre, J. A., & Reddy, R. (2015). Glutamate imaging (GluCEST) lateralizes epileptic foci in nonlesional temporal lobe Epilepsy. *Science Translational Medicine*, 7(309), 309ra161-309ra161. https://doi.org/10.1126/scitranslmed.aaa7095

Eid, T., Thomas, M. J., Spencer, D. D., Rundén-Pran, E., Lai, J. C. K., Malthankar, G. V., Kim, J. H., Danbolt, N. C., Ottersen, O. P., & Lanerolle, N. C. D. (2004). Loss of glutamine synthetase in the human epileptogenic hippocampus: Possible mechanism for raised extracellular glutamate in mesial temporal lobe epilepsy. *Lancet*, 363(9402), 28–37. https://doi.org/10.1016/s0140-6736(03)15166-5

Elsharkawy, A. E., Alabbasi, A. H., Pannek, H., Oppel, F., Schulz, R., Hoppe, M., Hamad, A. P., Nayel, M., Issa, A., & Ebner, A. (2009). Long-term outcome after temporal lobe epilepsy surgery in 434 consecutive adult patients: Clinical article. *Journal of Neurosurgery*, 110(6), 1135–1146. https://doi.org/10.3171/2008.6.jns17613

Fazel, S., Wolf, A., Långström, N., Newton, C. R., & Lichtenstein, P. (2013). Premature mortality in epilepsy and the role of psychiatric comorbidity: A total population study. *The Lancet*, 382(9905), 1646–1654. https://doi.org/10.1016/S0140-6736(13)60899-5

Gonen, O. M., Moffat, B. A., Desmond, P. M., Lui, E., Kwan, P., & O'Brien, T. J. (2020). Seven-tesla quantitative magnetic resonance spectroscopy of glutamate, γ-aminobutyric acid, and glutathione in the posterior cingulate cortex/Precuneus in patients with epilepsy. *Epilepsia*, 61(12), 2785–2794. https://doi.org/10.1111/epi.16731

Hadar, P. N., Kini, L. G., Nanga, R. P. R., Shinohara, R. T., Chen, S. H., Shah, P., Wisse, L. E. M., Elliott, M. A., Hariharan, H., Reddy, R., Detre, J. A., Stein, J. M., Das, S., & Davis, K. A. (2021). Volumetric glutamate imaging (GluCEST) using 7T MRI can lateralize nonlesional temporal lobe epilepsy: A preliminary study. *Brain and Behavior*, 11(8), e02134. https://doi.org/10.1002/brb3.2134

Kang, J. Y., Wu, C., Tracy, J., Lorenzo, M., Evans, J., Nei, M., Skidmore, C., Mintzer, S., Sharan, A. D., & Sperling, M. R. (2016). Laser interstitial thermal therapy for medically intractable mesial temporal lobe Epilepsy. *Epilepsia*, 57(2), 325–334. https://doi.org/10.1111/epi.13284

Keller, S. S., & Roberts, N. (2008). Voxel-based morphometry of temporal lobe epilepsy: An introduction and review of the literature. *Epilepsia*, 49(5), 741–757. https://doi.org/10.1111/j.1528-1167.2007.01485.x

Le, S., Ho, A. L., Fisher, R. S., Miller, K. J., Henderson, J. M., Grant, G. A., Meador, K. J., & Halpern, C. H. (2018). Laser interstitial thermal therapy (LITT): Seizure outcomes for refractory mesial temporal lobe epilepsy. *Epilepsy & Behavior*, 89, 37–41. https://doi.org/10.1016/j.yebeh.2018.09.040

Liu, M., Concha, L., Lebel, C., Beaulieu, C., & Gross, D. W. (2012). Mesial temporal sclerosis is linked with more widespread white matter changes in temporal lobe epilepsy. *NeuroImage: Clinical*, 1(1), 99–105. https://doi.org/10.1016/j.nicl.2012.09.010

Passarelli, V., Castro-Lima Filho, H., Adda, C. C., Preturlon-Santos, A. P., Valerio, R. M., Jorge, C. L., Puglia, P., Lyra, K., Otaduy, M. G., Wen, H.-T., & Castro, L. H. (2015). Contralateral ictal electrographic involvement is associated with decreased memory performance in unilateral mesial temporal sclerosis. *Journal of the Neurological Sciences*, 359(1–2), 241–246. https://doi.org/10.1016/j.jns.2015.11.008

Pimentel-Silva, L. R., Casseb, R. F., Cordeiro, M. M., Campos, B. A. G., Alvim, M. K. M., Rogerio, F., Yasuda, C. L., & Cendes, F. (2020). Interactions between in vivo neuronal-glial markers, side of hippocampal sclerosis, and pharmacoresponse in temporal lobe Epilepsy. *Epilepsia*, 61(5), 1008–1018. https://doi.org/10.1111/epi.16509

Princich, J. P., Donnelly-Kehoe, P. A., Deleglise, A., Vallejo-Azar, M. N., Pascariello, G. O., Seoane, P., Veron Do Santos, J. G., Collavini, S., Nasimbera, A. H., & Kochen, S. (2021). Diagnostic performance of MRI volumetry in epilepsy patients with hippocampal sclerosis supported through a random Forest automatic classification algorithm. *Frontiers in Neurology*, *12*.

Scharfman, H. E. (2019). The dentate gyrus and temporal lobe Epilepsy: An "exciting" era. *Epilepsy Currents*, *19*(4), 249–255. https://doi.org/10.1177/1535759719855952

Scheffer, I. E., Berkovic, S., Capovilla, G., Connolly, M. B., French, J., Guilhoto, L., Hirsch, E., Jain, S., Mathern, G. W., Moshé, S. L., Nordli, D. R., Perucca, E., Tomson, T., Wiebe, S., Zhang, Y., & Zuberi, S. M. (2017). ILAE classification of the epilepsies: Position paper of the ILAE commission for classification and terminology. *Epilepsia*, *58*(4), 512–521. https://doi.org/10.1111/epi.13709

Shah, P., Bassett, D. S., Wisse, L. E. M., Detre, J. A., Stein, J. M., Yushkevich, P. A., Shinohara, R. T., Elliott, M. A., Das, S. R., & Davis, K. A. (2019). Structural and functional asymmetry of medial temporal subregions in unilateral temporal lobe epilepsy: A 7T MRI study. *Human Brain Mapping*, *40*(8), 2390–2398. https://doi.org/10.1002/hbm.24530

Shah, P., Bassett, D. S., Wisse, L. E. M., Detre, J. A., Stein, J. M., Yushkevich, P. A., Shinohara, R. T., Pluta, J. B., Valenciano, E., Daffner, M., Wolk, D. A., Elliott, M. A., Litt, B., Davis, K. A., & Das, S. R. (2018). Mapping the structural and functional network architecture of the medial temporal lobe using 7T MRI. *Human Brain Mapping*, *39*(2), 851–865. https://doi.org/10.1002/hbm.23887

Spencer, S. S., Berg, A. T., Vickrey, B. G., Sperling, M. R., Bazil, C. W., Shinnar, S., Langfitt, J. T., Walczak, T. S., Pacia, S. V., & The Multicenter Study of Epilepsy Surgery. (2005). Predicting long-term seizure outcome after Resective Epilepsy surgery: The multicenter study. *Neurology*, *65*(6), 912–918. https://doi.org/10.1212/01.wnl.0000176055.45774.71

Stephen, L. J., Kwan, P., & Brodie, M. J. (2001). Does the cause of localisation-related epilepsy influence the response to antiepileptic drug treatment? *Epilepsia*, *42*(3), 357–362. https://doi.org/10.1046/j.1528-1157.2001.29000.x

Tamminga, C. A., Southcott, S., Sacco, C., Wagner, A. D., & Ghose, S. (2012). Glutamate dysfunction in hippocampus: Relevance of dentate gyrus and CA3 signaling. *Schizophrenia Bulletin*, *38*(5), 927–935. https://doi.org/10.1093/schbul/sbs062

Téllez-Zenteno, J. F.; Hernández-Ronquillo, L. A review of the epidemiology of temporal lobe Epilepsy. *Epilepsy Research and Treatment* 2011, *2012*, e630853. https://doi.org/10.1155/2012/630853, 1, 5.

Thom, M. (2014). Review: Hippocampal sclerosis in epilepsy—A neuropathology review. *Neuropathology and Applied Neurobiology*, *40*(5), 520–543. https://doi.org/10.1111/nan.12150

Wieser, H.-G., Epilepsy, & ILAE Commission on Neurosurgery of Epilepsy. (2004). Mesial temporal lobe epilepsy with hippocampal sclerosis. *Epilepsia*, *45*(6), 695–714. https://doi.org/10.1111/j.0013-9580.2004.09004.x

Yushkevich, P. A., Piven, J., Hazlett, H. C., Smith, R. G., Ho, S., Gee, J. C., & Gerig, G. (2006). User-guided 3D active contour segmentation of anatomical structures: Significantly improved efficiency and reliability. *NeuroImage*, *31*(3), 1116–1128. https://doi.org/10.1016/j.neuroimage.2006.01.015

Yushkevich, P. A., Pluta, J. B., Wang, H., Xie, L., Ding, S., Gertje, E. C., Mancuso, L., Kliot, D., Das, S. R., & Wolk, D. A. (2015). Automated volumetry and regional thickness analysis of hippocampal subfields and medial temporal cortical structures in mild cognitive impairment. *Human Brain Mapping*, *36*(1), 258–287. https://doi.org/10.1002/hbm.22627

Zack, M. M., & Rosemarie, R. (2017). National and state estimates of the numbers of adults and children with active epilepsy: United States, 2015. *MMWR. Morbidity and Mortality Weekly Report*, *66*, 821–825. https://doi.org/10.15585/mmwr.mm6631a1

SUPPORTING INFORMATION

Additional supporting information can be found online in the Supporting Information section at the end of this article.